Letter

Thermal Hall effect in a van der Waals triangular magnet $FeCl_2$

Chunqiang Xu,[1,2] Caitlin Carnahan,[3] Heda Zhang,[1] Milos Sretenovic,[1] Pengpeng Zhang,[1] Di Xiao,[4] and Xianglin Ke[1]

[1]*Department of Physics and Astronomy, Michigan State University, East Lansing, Michigan 48824-2320, USA*

[2]*School of Physical Science and Technology, Ningbo University, Ningbo 315211, China*

[3]*Department of Physics, Carnegie Mellon University, Pittsburgh, Pennsylvania 15213, USA*

[4]*Department of Materials Science and Engineering and Department of Physics, University of Washington, Seattle, Washington 98195, USA*

(Received 10 June 2022; revised 24 January 2023; accepted 26 January 2023; published 6 February 2023)

Thermal transport is a pivotal probe for studying low-energy, charge-neutral quasiparticles in insulating magnets. In this Letter, we report an observation of large magnetothermal conductivity and thermal Hall effect (THE) in a van der Waals antiferromagnet $FeCl_2$. The magnetothermal conductivity reaches over ∼700%, indicating strong magnon-phonon coupling. Furthermore, we find an appreciable thermal Hall signal which changes sign concurrently with the spin-flip transition from the antiferromagnetic state to the polarized ferromagnetic state. Our theoretical calculations suggest that, in addition to the Berry curvature induced at the anticrossing points of the hybridized magnon and acoustic phonon modes of $FeCl_2$, other mechanisms are needed to account for the magnitude of the observed THE.

DOI: 10.1103/PhysRevB.107.L060404

I. INTRODUCTION

Thermal transport is an important technique for studying low-energy excitations of quantum materials. For instance, the thermal Hall effect (THE), i.e., the generation of a transverse heat current carried by charge-neutral quasiparticles in the presence of a longitudinal temperature gradient, has been attracting more and more attention since the experimental observation of THE in the paramagnetic insulator $Tb_3Ga_5O_{12}$ reported by Strohm *et al.* in 2005 [1]. In particular, the THE may be used to probe the characteristic features of emergent quantum phases. For instance, THE measurements provide pivotal evidence of topological magnons in magnetic insulators [2–4], chiral phonons in cuprate superconductors [5,6], and potential Majorana-fermions in Kitaev quantum spin liquid candidates [7–10].

In magnetic solids with strong magnetoelastic coupling, magnon-phonon coupling can modify the features of both magnetic excitations and lattice vibrations. For instance, magnons and phonons can scatter off one another, leading to the shortened lifetimes and the resulting suppression of heat conduction carried by these quasiparticles. Furthermore, magnon and phonon modes may hybridize, leading to the emergence of coherent quasiparticles known as magnon polarons [11–13]. Compared to the band structures of noninteracting magnon and phonon modes which cross each other, a salient characteristic of the magnon-phonon hybridized excitations is the appearance of anticrossing points leading to a gap opening at the intersections of magnon and phonon dispersions. Recently, it has been shown that these anticrossing points give rise to Berry curvature hot spots [4,14–18]. As a result, magnon polarons may exhibit nontrivial topological character with the hybridized bands carrying nonzero Chern numbers, which are then anticipated to yield a THE [15–18]. Despite the increasing theoretical attention and potential applications in spin caloritronics and magnon spintronics [19], experimental realization of magnon polaron driven THE is very rare.

In this Letter, we report the observation of large magnetothermal conductivity and THE in a van der Waals (vdW) antiferromagnetic insulator $FeCl_2$ hosting a triangular magnetic lattice. The magnetothermal conductivity reaches over ∼ 700%, indicating strong magnon-phonon coupling. The THE increases with magnetic field prior to the spin-flip transition from the antiferromagnetic state to the polarized ferromagnetic state, at which the THE exhibits a sign change followed by a decrease in magnitude upon further increasing the field. Our theoretical calculations suggest that magnon polarons resulting from the hybridized magnon and acoustic phonon modes in $FeCl_2$ can be associated with the observed THE. The discrepancy in the magnitude of thermal Hall conductivity between the experimental data and the theoretical calculation indicates the possibility of other contributing mechanisms which call for future studies.

II. RESULTS AND DISCUSSION

$FeCl_2$ crystalizes in the space group $R\bar{3}m$ (No. 166) at room temperature with lattice constants $a = b = 3.600(3)$ Å, $c = 17.539(2)$ Å and crystalline angles of $\alpha = \beta = 90°$, $\gamma = 120°$ [20]. As illustrated in Figs. 1(a) and 1(b), $FeCl_2$ is a vdW material with the iron atoms forming a triangle structure in the *ab* plane. Previous neutron measurements showed that $FeCl_2$ is an *A*-type antiferromagnet below $T_N \sim 23.5$ K with neighboring ferromagnetic planes weakly coupled antiferromagnetically along the *c* axis and the magnetic easy axis along *c* [21,22]. Owing to the strong spin-orbit coupling, its magnetic excitation exhibits a large single-ion anisotropy gap of

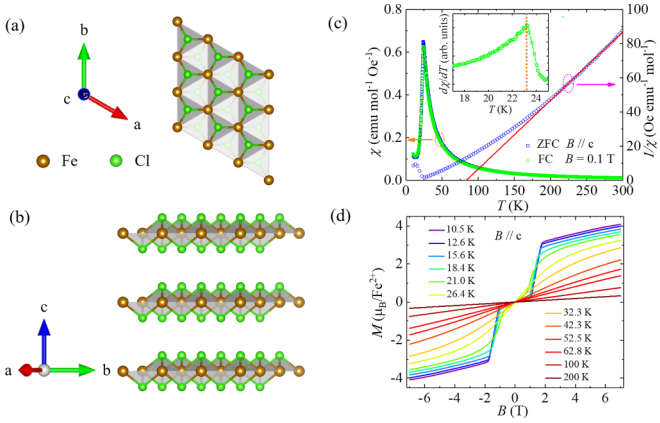

FIG. 1. Crystal structure and magnetization of $FeCl_2$. (a,b) Schematic crystal structure of $FeCl_2$ viewed along two different perspectives. (c) Temperature dependence of dc magnetic susceptibility χ with 0.1 T magnetic field applied along the c axis. The red solid linear line is the Curie-Weiss fitting and the inset is an expanded view of $d\chi/dT$ at low temperatures. (d) Isothermal magnetization curves measured at various temperatures.

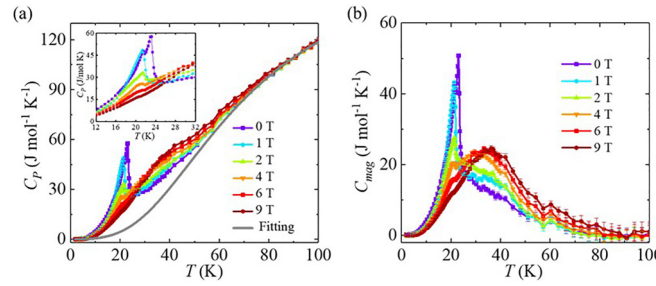

FIG. 2. Specific heat of $FeCl_2$. (a) Temperature dependence of specific heat C_p measured at various magnetic fields. The gray curve is a fitting based on a Debye equation for the phonon contribution. The inset shows an expanded view. (b) Temperature dependence of the extracted magnetic specific heat C_{mag}.

~ 2.2 meV, and its magnon dispersions can be nicely described using the spin wave theory on a two-dimensional ferromagnet with effective $S = 1$ moment [23]. Previous theoretical studies suggested that the magnon and phonon modes may hybridize near the zone center in this system [24], motivating us to investigate the thermal Hall effect. Detailed information regarding the material synthesis and experimental methods can be found in the Supplemental Material [25] which also includes Refs. [26–28].

Figure 1(c) plots the temperature dependence of dc magnetic susceptibility χ and reciprocal $1/\chi$ of $FeCl_2$ with a magnetic field of 0.1 T applied along the c axis. One can clearly see a large drop in χ below ~ 23.2 K (see inset) in both zero field cooled (ZFC) and field-cooled (FC) measurements, indicative of an antiferromagnetic transition. The Curie temperature θ_{CW} extracted from the Curie-Weiss fit above 220 K is found to be $\sim$84 K, and the effective magnetic moment μ_{eff} is about 4.46 μ_B which is slightly smaller than the spin-only value of 4.90 μ_B for Fe^{2+} in a $3d^6$ configuration. Although $FeCl_2$ is antiferromagnetic, the positive sign of θ_{CW} stems from the dominant ferromagnetic interactions within the ab plane. The isothermal magnetization $M(H)$ measured at various temperatures is shown in Fig. 1(d). Below T_N, the magnetization increases sharply when the magnetic field reaches a critical value of $B_c \sim 1.5$ T, characteristic of spin-flip transition, above which the system becomes a polarized ferromagnet, which is consistent with previous reports [29–31]. The small B_c of the transition indicates weak antiferromagnetic interlayer couplings, affirming the vdW nature of this system.

Figure 2(a) and the inset present the temperature dependence of specific heat C_P of $FeCl_2$ measured at various magnetic fields. At zero magnetic field, an anomaly occurs at 23.5 K, signaling the magnetic phase transition. Note that there is a small, additional anomaly near 21 K, which is not seen in the χ (T) data discussed above and in the previous neutron diffraction studies [21,22]. Such an anomaly was observed in two samples grown in different batches. It is presumably associated with the collapse of the entire magnon branches into a continuum scattering between 21 K (0.9 T_N) and T_N as revealed by the inelastic neutron scattering studies [23]. In the presence of a magnetic field, the anomaly associated with antiferromagnetic phase transitions is suppressed, while the magnitude of C_P increases above T_N compared to the values obtained at zero field. As an attempt to extract the magnetic heat capacity C_{mag}, using a Debye equation we fitted the $C_P(T)$ data measured at zero field between 2 and 100 K excluding the 7–80 K range. The thus-obtained phonon contribution to the heat capacity, shown as the gray curve in Fig. 2(a), was then subtracted from C_P data measured at various magnetic fields. The extracted $C_{mag}(T)$ curves are plotted in Fig. 2(b) where broad peaks around 35 K (above T_N) are observed whose magnitude increases in the presence of a magnetic field up to 9 T. This feature suggests the onset of ferromagnetic correlation within the triangular planes which precedes the three-dimensional long-range antiferromagnetic order at T_N due to the weak antiferromagnetic interlayer coupling [23]. In the presence of a magnetic field, the associated Zeeman energy competes with the thermal energy and antiferromagnetic interlayer coupling. This may be responsible for enhancing the spin correlation between the triangular planes, thus leading to an increase in heat capacity above T_N. Note that the magnitude of heat capacity can be off by a factor of 2 due to the small mass ($\sim$0.3 mg) of the sample measured that is close to the uncertainty of the scale.

Figure 3(a) illustrates the schematic of the experimental setup for thermal transport measurements. Three temperature sensors and one heater were used. The heat current ($\boldsymbol{J}_Q$) was applied in the ab plane and the sign convention of κ_{xx} and κ_{xy} was determined by $\Delta T_{xx} = T_2 - T_1$ (in the direction of $\boldsymbol{J}_Q$) and $\Delta T_{yx} = T_3 - T_1$ (in the direction of $\boldsymbol{B} \times \boldsymbol{J}_Q$), respectively (see Fig. S1 [25]). The magnetic field was applied along the c axis. Figure 3(b) shows the temperature dependence of the longitudinal thermal conductivity $\kappa_{xx}(T)$ measured at various magnetic fields. In insulating magnetic solids, the thermal conduction is carried by magnons and phonons; thus $\kappa_{xx} = \kappa_{xx}^m + \kappa_{xx}^p$ where κ_{xx}^m and κ_{xx}^p represent the magnon and phonon contribution to the thermal conductivity, respectively. In the absence of a magnetic field, no anomalous feature in $\kappa_{xx}(T)$ is observed at T_N as would be expected from an

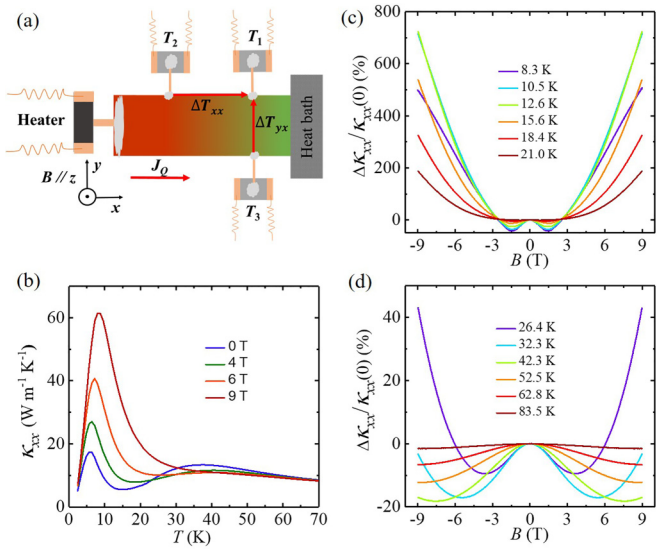

FIG. 3. Thermal conductivity of $FeCl_2$. (a) A schematic of the experimental setup for thermal transport measurements. (b) Thermal conductivity κ_{xx} as a function of temperature measured with various magnetic fields. (c,d) Magnetothermal conductivity measured at various temperatures. The magnetic field is applied along the c axis.

exchange-dominated magnetostriction. Instead, an anomalous dip in $\kappa_{xx}(T)$ between two broad peaks was observed below T_N, consistent with early reports [32–34], which implies phonon scattering by magnons. Below the low-temperature peak around 5.6 K, κ_{xx} is dominated by κ_{xx}^p because of the small population of magnons due to the single-ion anisotropy gap of ~ 2.2 meV at the zone center of magnetic excitations [23]. In the intermediate-temperature region, the population of thermally populated magnons increases, which scatters phonons via the strong magnon-phonon coupling and results in a decrease in κ_{xx}^p. Such a decrease in κ_{xx}^p even overcomes the thermal contribution of magnons, leading to the reduction of the total κ_{xx}. As the temperature further increases and approaches T_N, magnons become less coherent with a decrease in magnon lifetime as inferred from inelastic neutron scattering studies [23]. Thus, the phonon scattering by magnons decreases, which then increases the total κ_{xx} again until above 40 K at which point the umklapp scattering dominates leading to a decrease in κ_{xx}. A similar argument was made in Ref. [30] to account for the zero-field $\kappa_{xx}(T)$ features. With an applied magnetic field larger than B_c, $FeCl_2$ becomes a polarized ferromagnet and the magnon gap value increases with increasing magnetic field, giving rise to the reduction of magnon population. As a result, magnon-phonon scattering is suppressed and the phonon mean free path increases, resulting in an increase in κ_{xx}^p and thus total κ_{xx} in the low-temperature region. On the other hand, as suggested by the specific heat measurement shown in Fig. 2 and discussed above, ferromagnetic correlation within the triangular planes sets in above T_N. An application of magnetic field enhances three-dimensional ferromagnetic correlation, which leads to more coherent magnons that scatter phonons and consequently decrease the total κ_{xx} compared to κ_{xx} measured at zero field. Future inelastic neutron scattering studies of $FeCl_2$ in the presence of a magnetic field are desirable to shed light on this.

Figures 3(c) and 3(d) show the magnetothermal conductivity, which is defined as $[\kappa_{xx}(B) - \kappa_{xx}(0)] \times 100\%/\kappa_{xx}(0)$, as a function of magnetic field measured at various temperatures. One can see that $FeCl_2$ exhibits very large magnetothermal conductivity, reaching over 700% around 10 K at 9 T, again suggesting strong phonon scattering by magnons which is suppressed in the presence of a high field as discussed above. The magnetic field dependence of magnon bands of $FeCl_2$ is illustrated in Fig. S10 in the Supplemental Material [25]. Below T_N, at zero magnetic field $FeCl_2$ has two magnon bands that are degenerate. An application of a magnetic field smaller than B_c, when $FeCl_2$ remains antiferromagnetic, breaks the degeneracy of the magnon bands by shifting down one magnon branch in energy while pushing up the other magnon branch due to the Zeeman interaction. As a result, the phonon scattering by magnons is slightly enhanced and the resultant κ_{xx}^p and the total κ_{xx} decrease, as shown in Fig. 3(c). Above B_c, as discussed above, $FeCl_2$ becomes ferromagnetic via the spin-flip transition and the magnon gap increases with magnetic field. Thus, the phonon scattering by magnons is suppressed due to the decrease in the magnon population, leading to positive magnetothermal conductivity. As shown in Fig. 3(d), similar features in magnetothermal conductivity are observed above T_N, although with much smaller magnitude, which is presumably ascribed to the (para)magnons associated with ferromagnetic correlation with the triangular planes that diminishes around 80 K.

Next, we present the THE observed in $FeCl_2$. To unambiguously validate the intrinsic nature of the measured thermal Hall signal, we have measured the thermal Hall signal, sweeping the magnetic field from −9 to 9 T and back, and following the procedure reported in Refs. [3,35] to examine its hysteretic behavior. In addition, measurements were also performed using different heating powers and on different samples to ensure the intrinsic nature of the THE and its reproducibility. Detailed procedures for extracting the thermal Hall signal and the thermal transport data measured on another sample are described in the Supplemental Material (Figs. S2–S9) [25].

Figure 4(a) presents the field dependent thermal Hall conductivity κ_{xy} measured at various temperatures. A large THE is clearly observed. Below T_N, κ_{xy} increases with increasing magnetic field and then sharply switches sign near 1.5 T which coincides with the spin-flip transition at B_c, as also shown in Fig. S7 [25]. Upon increasing the temperature, the magnitude of κ_{xy} just above B_c increases, reaching 0.05 W m^{-1} K^{-1} with a large thermal Hall angle ($\theta_{th} = \kappa_{xy}/\kappa_{xx}$) of 0.008 at $T \sim$ 18 K (shown in Fig. S6 [25]). After the sign change, the magnitudes of both κ_{xy} and θ_{th} decrease when further increasing the magnetic field. These features exclude the possibility that the observed thermal Hall signal in $FeCl_2$ (1) is purely driven by phonons as reported in nonmagnetic $SrTiO_3$ [36] since one would expect κ_{xy} monotonically increases with magnetic field; (2) is driven by phonon THE induced by the internal magnetic field of magnetization since no sign change in κ_{xy} would be expected. In addition, as will be discussed next, the observed thermal Hall signal cannot be ascribed to topological magnons either, since the magnon bands are topologically

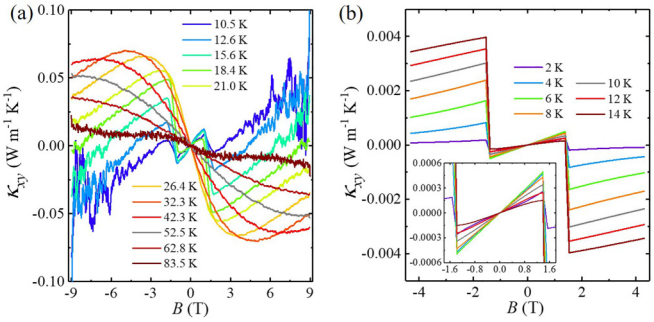

FIG. 4. Thermal Hall conductivity of $FeCl_2$. (a) Magnetic field dependence of thermal hall conductivity κ_{xy} measured at various temperatures. (b) The calculated bilayer thermal Hall conductivity with magnon-phonon coupling constant $g = 1.0$ (see Supplemental Material [25] for details) assuming a transition to an induced ferromagnetic phase at the critical field of $B_c = 1.5$ T. Below B_c, $\kappa_{xy} = (\kappa_{xy}^{\uparrow} + \kappa_{xy}^{\downarrow})/2$ and above B_c, $\kappa_{xy} = \kappa_{xy}^{\uparrow}$. Inset: an expanded view of the temperature dependence in the antiferromagnetic weak-field region.

trivial. Instead, the observed THE in $FeCl_2$ can be associated with the magnon-phonon hybridization [24].

To theoretically study the THE in $FeCl_2$ below T_N, we first consider the monolayer triangular lattice model and take into account the magnon-phonon coupling. The associated Hamiltonian, parameters, and detailed calculations are discussed in Sec. V in the Supplemental Material [25]. As shown in Fig. S11, with the inclusion of the phonon bands and the introduction of magnon-phonon coupling, a gap opens between the hybridized bands. These hybridized bands exhibit nontrivial topological Berry curvature, from which κ_{xy} of the ferromagnetic monolayer triangular lattice may be calculated (see Fig. S12 with additional details in the Supplemental Material [25]).

The THE driven by magnons [37] and magnon polarons [38] has been very recently studied theoretically in honeycomb antiferromagnets, and shown to be sensitively dependent on the external magnetic field which can induce both topological and magnetic phase transitions. Such a dependence on the magnetic field is similarly expected to influence the profile of the thermal Hall signal in antiferromagnetically coupled $FeCl_2$ bilayers. To incorporate the effects of the weak antiferromagnetic interlayer interaction in $FeCl_2$, we employ an effective bilayer approach where, in the antiferromagnetic phase, the total thermal Hall conductivity κ_{xy} is given by $\kappa_{xy} = (\kappa_{xy}^{\uparrow} + \kappa_{xy}^{\downarrow})/2$ with $\kappa_{xy}^{\uparrow(\downarrow)}$ being the thermal Hall conductivity calculated from $+(-)\hat{B}$-polarized magnons in the monolayer calculation. In the presence of a weak external field, this approach assumes decoupled magnon modes of opposing polarization in the bilayers, an assumption that is predicated on the weak interlayer coupling and strong single-ion anisotropy exhibited by $FeCl_2$. Beyond the critical field B_c, the system becomes a polarized ferromagnet where κ_{xy} is simply given by $\kappa_{xy}^{\uparrow}$.

The calculated thermal Hall conductivity due to magnon-phonon coupling in bilayer $FeCl_2$ is shown in Fig. 4(b) as a function of magnetic field for various temperatures. The critical field B_c at which the induced ferromagnetic phase begins is approximated from the experimental data. A striking similarity with experimental results is observed in the field dependence of the calculated bilayer κ_{xy}, especially regarding the sign change at B_c. As illustrated in Fig. S10 [25], at zero field, the $\uparrow$ and $\downarrow$ magnon bands are degenerate and, since these systems are related to one another through a π rotation about the x axis, their thermal Hall conductivities cancel each other exactly. Introduction of a small external field breaks the degeneracy of the $\uparrow$ / $\downarrow$ magnon bands, leading to suppression of the $\uparrow$ magnon population and allowing the contribution from the $\downarrow$ magnon band to dominate. In the induced ferromagnetic phase right above B_c, however, only the $\uparrow$ magnon band with an enhanced population remains to determine κ_{xy}, leading to a sign change in the overall thermal Hall signal with an increase in the magnitude of κ_{xy}. As the external field continues to increase in magnitude, κ_{xy} is further suppressed as the magnon band shifts higher in energy, increasing the energy of magnon-phonon hybridization and reducing the magnon population. These theoretical results qualitatively support the notion that the THE is partially contributed by magnon-phonon hybridization in $FeCl_2$, and the characteristic sign change in κ_{xy} is indicative of the transition from the layered antiferromagnetic phase to the induced ferromagnetic phase. We note that there is a quantitative discrepancy in κ_{xy} between the experimental data and the theoretical calculation, particularly at higher temperatures. Such a discrepancy may be attributed to features that are not included in the model (e.g., coupling with additional phonon modes, higher-order fluctuation terms, etc.). In addition, our theoretical results do not discount the possibility of contributions to the THE from other mechanisms such as magnon-phonon scattering. Unfortunately, the contribution from magnon-phonon scattering to the THE is seldom discussed in the literature, and warrants future studies. While the extent to which magnon-phonon hybridization contributes to the observed thermal Hall signal cannot be established quantitatively with the present methods, we believe that the theoretical calculation presented here serves as a proof of concept model providing a qualitative description of the essential physics underlying the shape of the κ_{xy} signal.

III. CONCLUSION

In conclusion, we report the observation of large magnetothermal conductivity and THE in a vdW antiferromagnet $FeCl_2$, elucidating strong magnon-phonon coupling in $FeCl_2$. The thermal Hall signal changes the sign upon the spin-flip transition from the antiferromagnetic state to the polarized ferromagnetic state. The observed THE is in qualitative agreement with the THE arising from the Berry curvature at the anticrossing points of hybridized magnon and phonon modes, suggesting that the THE is partially contributed from magnon polarons. Nevertheless, the discrepancy in the magnitude of the THE between the calculation result and experimental data suggests that other mechanisms can also play a role, which calls for future theoretical studies.

Data for the figures presented in this paper are available at [39].

ACKNOWLEDGMENTS

H.Z., M.S., and X.K. acknowledge the financial support by the U.S. Department of Energy, Office of Science, Office of Basic Energy Sciences, Materials Sciences and Engineering Division under Contract No. DE-SC0019259. X.K. also acknowledges the financial support by the National Science Foundation (Grant No. DMR-2219046). X.K. appreciates the insightful discussion with Professor S. D. Mahanti. P.Z. acknowledges the financial support by the National Science Foundation (Grant No. DMR-2112691). C.C. and D.X. are supported by AFOSR MURI 2D MAGIC (Grant No. FA9550-19-1-0390). C.X. is partially supported by the Start-up funds at Michigan State University.

[1] C. Strohm, G. L. J. A. Rikken, and P. Wyder, Phenomenological Evidence for the Phonon Hall Effect, Phys. Rev. Lett. **95**, 155901 (2005).

[2] Y. Onose, T. Ideue, H. Katsura, Y. Shiomi, N. Nagaosa, and Y. Tokura, Observation of the magnon Hall effect, Science **329**, 297 (2010).

[3] M. Hirschberger, R. Chisnell, Y. S. Lee, and N. P. Ong, Thermal Hall Effect of Spin Excitations in a Kagome Magnet, Phys. Rev. Lett. **115**, 106603 (2015).

[4] H. Zhang, C. Xu, C. Carnahan, M. Sretenovic, N. Suri, D. Xiao, and X. Ke, Anomalous Thermal Hall Effect in an Insulating van der Waals Magnet, Phys. Rev. Lett. **127**, 247202 (2021).

[5] G. Grissonnanche, A. Legros, S. Badoux, E. Lefrançois, V. Zatko, M. Lizaire, F. Laliberté, A. Gourgout, J. S. Zhou, S. Pyon, T. Takayama, H. Takagi, S. Ono, N. Doiron-Leyraud, and L. Taillefer, Giant thermal Hall conductivity in the pseudogap phase of cuprate superconductors, Nature (London) **571**, 376 (2019).

[6] G. Grissonnanche, S. Thériault, A. Gourgout, M. E. Boulanger, E. Lefrançois, A. Ataei, F. Laliberté, M. Dion, J. S. Zhou, S. Pyon, T. Takayama, H. Takagi, N. Doiron-Leyraud, and L. Taillefer, Chiral phonons in the pseudogap phase of cuprates, Nat. Phys. **16**, 1108 (2020).

[7] Y. Kasahara, T. Ohnishi, Y. Mizukami, O. Tanaka, S. Ma, K. Sugii, N. Kurita, H. Tanaka, J. Nasu, Y. Motome, T. Shibauchi, and Y. Matsuda, Majorana quantization and half-integer thermal quantum Hall effect in a Kitaev spin liquid, Nature (London) **559**, 227 (2018).

[8] Y. Kasahara, K. Sugii, T. Ohnishi, M. Shimozawa, M. Yamashita, N. Kurita, H. Tanaka, J. Nasu, Y. Motome, T. Shibauchi, and Y. Matsuda, Unusual Thermal Hall Effect in a Kitaev Spin Liquid Candidate α-$RuCl_3$, Phys. Rev. Lett. **120**, 217205 (2018).

[9] J. A. N. Bruin, R. R. Claus, Y. Matsumoto, N. Kurita, H. Tanaka, and H. Takagi, Robustness of the thermal Hall effect close to half-quantization in α-$RuCl_3$, Nat. Phys. **18**, 401 (2022).

[10] T. Yokoi, S. Ma, Y. Kasahara, S. Kasahara, T. Shibauchi, N. Kurita, H. Tanaka, J. Nasu, Y. Motome, C. Hickey, S. Trebst, and Y. Matsuda, Half-integer quantized anomalous thermal Hall effect in the Kitaev material candidate α-$RuCl_3$. Science **373**, 568 (2021).

[11] C. Kittel, Interaction of spin waves and ultrasonic waves in ferromagnetic crystals, Phys. Rev. **110**, 836 (1958).

[12] A. P. Cracknell, A group theory study of selection rules for magnon-phonon interactions in ferromagnetic hcp metals, J. Phys. F: Met. Phys **4**, 466 (1974).

[13] B. Flebus, K. Shen, T. Kikkawa, K.-i. Uchida, Z. Qiu, E. Saitoh, R. A. Duine, and G. E. W. Bauer, Magnon-polaron transport in magnetic insulators, Phys. Rev. B **95**, 144420 (2017).

[14] E. Thingstad, A. Kamra, A. Brataas, and A. Sudbø, Chiral Phonon Transport Induced by Topological Magnons, Phys. Rev. Lett. **122**, 107201 (2019).

[15] X. Zhang, Y. Zhang, S. Okamoto, and D. Xiao, Thermal Hall Effect Induced by Magnon-Phonon Interactions, Phys. Rev. Lett. **123**, 167202 (2019).

[16] G. Go, S. K. Kim, and K.-J. Lee, Topological Magnon-Phonon Hybrid Excitations in Two-Dimensional Ferromagnets with Tunable Chern Numbers, Phys. Rev. Lett. **123**, 237207 (2019).

[17] S. Zhang, G. Go, K.-J. Lee, and S. K. Kim, SU(3) Topology of Magnon-Phonon Hybridization in 2D Antiferromagnets, Phys. Rev. Lett. **124**, 147204 (2020).

[18] R. Takahashi and N. Nagaosa, Berry Curvature in Magnon-Phonon Hybrid Systems, Phys. Rev. Lett. **117**, 217205 (2016).

[19] D. A. Bozhko, V. I. Vasyuchka, A. V. Chumak, and A. A. Serga, Magnon-phonon interactions in magnon spintronics (Review article), Low Temp. Phys. **46**, 383 (2020).

[20] R. de Kouchkovsky and J. A. Nasser, X-ray investigation of magnetostriction in $FeCl_2$, J. Phys. **47**, 1741 (1986).

[21] M. K. Wilkinson, J. W. Cable, E. O. Wollan, and W. C. Koehler, Neutron diffraction investigations of the magnetic ordering in $FeBr_2$, $CoBr_2$, $FeCl_2$, and $CoCl_2$, Phys. Rev. **113**, 497 (1959).

[22] W. B. Yelon and R. J. Birgeneau, Magnetic properties of $FeCl_2$ in zero field. II. Long-range order, Phys. Rev. B **5**, 2615 (1972).

[23] R. J. Birgeneau, W. B. Yelon, E. Cohen, and J. Makovsky, Magnetic properties of $FeCl_2$ in zero field. I. excitaTions, Phys. Rev. B **5**, 2607 (1972).

[24] U. Balucani and A. Stasch, Hybrid excitations in layered iron halides, Phys. Rev. B **32**, 182 (1985).

[25] See Supplemental Material at http://link.aps.org/supplemental/10.1103/PhysRevB.107.L060404 for detailed information of material synthesis and experimental methods, thermal Hall measurements, and theoretical calculations, which includes Refs. [26–28].

[26] H. Lee, J. H. Han, and P. A. Lee, Thermal Hall effect of spins in a paramagnet, Phys. Rev. B **91**, 125413 (2015).

[27] R. Matsumoto and S. Murakami, Theoretical Prediction of a Rotating Magnon Wave Packet in Ferromagnets, Phys. Rev. Lett. **106**, 197202 (2011).

[28] E. Torun, H. Sahin, S. K. Singh, and F. M. Peeters, Stable half-metallic monolayers of $FeCl_2$, Appl. Phys. Lett. **106**, 192404 (2015).

[29] A. Ito and K. Ôno, Magnetization of $FeCl_2$ single crystal, J. Phys. Soc. Jpn. **20**, 784 (1965).

[30] I. S. Jacobs and P. E. Lawrence, Metamagnetic phase transitions and hysteresis in $FeCl_2$, Phys. Rev. **164**, 866 (1967).

[31] C. Binek, D. Bertrand, L. P. Regnault, and W. Kleemann, Magnetic neutron-scattering investigation of the field-induced Griffiths phase in $FeCl_2$, Phys. Rev. B **54**, 9015 (1996).

[32] M. D. Tiwari and P. N. Ram, Magnon-phonon interactions in the thermal conductivity of antiferromagnetic $FeCl_2$, J. Magn. Magn. Mater. **15–18**, 897 (1980).

[33] G. Laurence, Low-temperature thermal conductivity of $CdCl_2$ and $FeCl_2$ and critical magnetic scattering of phonons in $FeCl_2$, Phys. Lett. A **34**, 308 (1971).

[34] G. Laurence and D. Petitgrand, Thermal Conductivity and Magnon-Phonon Resonant Interaction in Antiferromagnetic $FeCl_2$, Phys. Rev. B **8**, 2130 (1973).

[35] P. Czajka, T. Gao, M. Hirschberger, P. Lampen-Kelley, A. Banerjee, J. Yan, D. G. Mandrus, S. E. Nagler, and N. P. Ong, Oscillations of the thermal conductivity in the spin-liquid state of α-$RuCl_3$, Nat. Phys. **17**, 915 (2021).

[36] X. Li, B. Fauqué, Z. Zhu, and K. Behnia, Phonon Thermal Hall Effect in Strontium Titanate, Phys. Rev. Lett. **124**, 105901 (2020).

[37] R. R. Neumann, A. Mook, J. Henk, and I. Mertig, Thermal Hall Effect of Magnons in Collinear Antiferromagnetic Insulators: Signatures of Magnetic and Topological Phase Transitions, Phys. Rev. Lett. **128**, 117201 (2022).

[38] B. Ma and G. A. Fiete, Antiferromagnetic insulators with tunable magnon-polaron Chern numbers induced by in-plane optical phonons, Phys. Rev. B **105**, L100402 (2022).

[39] https://doi.org/10.5281/zenodo.7595730.